

Detection of Paracetamol in Water and Urea in Artificial Urine with Gold Nanoparticle@Al Foil Cost-efficient SERS Substrate

Zhansaya MUKANOVA, Kristina GUDUN, Zarina ELEMESOVA, Laura KHAMKHASH, Ekaterina RALCHENKO, and Rostislav BUKASOV†

Chemistry Department, School of Science and Technology, Nazarbayev University, Kabanbay Batyr Ave. 53, Astana, 010000, Kazakhstan

We demonstrated that a cost-efficient, easy to prepare, hybrid SERS substrate-gold nanoparticles (AuNPs) on untreated Al foil (AIF) can effectively detect pharmaceuticals, such as paracetamol and clinical biomarkers, like urea in artificial urine. The limit of detection (LOD) for paracetamol on AuNPs on AIF is superior (0.1 vs. 1 mM) to the LOD reported for SERS detection of paracetamol in the literature. For SERS detection of urea in urine, AuNPs on both Al foil and Au film performed much better than AuNPs on glass, in terms of the concentration range, linearity and LOD. However, assay on AuNPs on AIF showed a better semi-logarithmic trendline with $R^2 = 0.98$ than an assay on AuNPs on Au film with $R^2 = 0.94$. They have comparable sensitivity with LOD 0.024 and 0.017 M, respectively. The limit of quantification (LOQ) of the former is 0.026 M, which makes it sufficient for the quantification of urea in urine at both normal and pathophysiological (0.03 – 0.15 M) concentration.

Keywords Surface enhanced Raman spectroscopy (SERS), Al foil, cost effective, paracetamol, urea, biomarker, urine, LOD, LOQ

(Received August 8, 2017; Accepted September 22, 2017; Published February 10, 2018)

Introduction

Since surface-enhanced Raman scattering (SERS) was reported about four decades by Fleischman *et al.*, this label-free, sensitive and rapid method with significant multiplexing potential has been in focus of expanding interest of the scientific community.¹⁻³ Increasing numbers of SERS applications in biosensing have been reported.⁴ Those include early medical diagnostics and reliable detection of major health threats for human (*e.g.* cancer, tuberculosis, *etc.*) and animals as well as chemical-warfare agents.^{5,6} For example, SERS sandwich immunoassays have shown an ultra-low limit of detection (1 pg/mL) for a prostate-specific antigen.⁷ By far most of the SERS applications use gold or silver nanoparticles as well as gold (*e.g.* commercial substrates such as Klarite) or silver nanostructures as the enhancing substrates. Those substrates, however, are usually expensive and require plasma (or piranha solution) cleaning due to relatively strong adsorption of thiolates and other organic compounds to the gold and silver surface.⁸ Also, even gold nanostructures, such as nanocrescents would change their shape, including the tip radius of curvature, if exposed to a buffer solution for just several hours,⁹ which is even more the case for silver triangular nano-pyramids prepared by Van Duyne group.¹⁰ Those changes in addition to the formation of an oxide film are likely to impact the SERS enhancement factors, making them less reproducible. Those considerations drive interest for SERS detection on hybrid substrates, which often may successfully

compete in terms of sensing parameters (LOD, SERS EF, *etc.*) with SERS detection on gold/silver films, or even gold/silver nanostructured substrates; for instance, it was demonstrated by the detection of melamine with LOD of 50 nM using silver nanoparticles at the surface of filter membrane.¹¹ Those substrates are typically made of silver (AgNPs) or gold nanoparticle set on the surface of non-metal (*e.g.* AgNPs on Si nanowires)¹² or non-noble metal substrates, such as, for instance, two penny coins, reported for the detection of 3 drugs by the Goodacre group.¹³ Concave gold nanocubes at the surface of Al-6063 alloy were used as the SERS substrate for the detection of Rhodamine 6G, Rose Bengal and crystal violet.¹⁴

Recently we reported a relatively inexpensive and simple method for a fabrication of hybrid SERS substrate using commercial gold nanoparticles drop-casted on untreated and unmodified Al foil.¹⁵ This substrate can be prepared in just 1 or 2 h using only micro-centrifuge as equipment. And can achieve relatively high analytical EFs of about 10^7 and a low LOD of about 0.1 – 0.2 nM for 4-nitrobenenethiol (NBT) and crystal violet. In the present paper, for the first time we explore biomedical applications of this hybrid substrate in SERS detection of widely used pharmaceutical paracetamol and important biomarker urea, often clinically detected in urine.

Urea tests are widely used in clinical analysis to evaluate a kidney activity, especially for renal patients, while dramatic changes in the level of urea indicate malnutrition.¹⁶ Chronic kidney disease is one of the major global health problems, because tens of million people are affected and millions of people are dying every year from it, while it is especially prevalent among the aging population (up to 35% over 70 years are effected).¹⁷ Detecting the renal dysfunction at early stages

† To whom correspondence should be addressed.
E-mail: rostislav.bukasov@nu.edu.kz

may significantly reduce the mortality rate from this condition. Because urea is the final product of protein catabolism, its concentration can be monitored in order to detect early kidney dysfunction. A few techniques, including SERS, have been reported to analyze urine and to quantify its metabolites. For instance, Wang *et al.* demonstrated the detection of creatinine in urine by using gold colloids as a SERS active substrate.¹⁸ Another study conducted by Choi and co-workers analyzed the detection of promethazine and urea in urine for allowing continuous monitoring of drug delivery and kidney function, respectively.¹⁹ The concentration of urea in human urine may vary significantly (daily excretion of 342 ± 67 mmol in 490 to 2690 mL urine).²⁰ The average concentration of urea in urine is reported to be ~ 333 mM. However, the its pathophysiological level of 30 – 150 mM can indicate lost kidney function.¹⁹ Therefore, the ideal target quantification concentration range of urea in urine is about 0.03 – 0.5 M.

The occurrence of pharmaceutical compounds, such as paracetamol and ibuprofen, in an aquatic environment has been recognized as one of the emerging issues in environmental chemistry.²¹ While SERS detection of both urea and paracetamol²² has been already reported in the literature, a direct comparison of commercial AuNPs@Al foil with those SERS substrates is possible. However, we still prepared, measured and analyzed data obtained with self-developed AuNPs@evaporated Au film and AuNPs@glass slides as two control substrates for the detection of urea in artificial urine.

Experimental

The experimental part is for the most part similar to that described in Gudun *et al.* publication.¹⁵ Hereafter its a brief description is given.

Reagents

Gold nanoparticles, 60 and 80 nm diameter, OD = 1 in PBS buffers were obtained from Sigma-Aldrich. Urea, lactic and citric acids, sodium bicarbonate, calcium chloride, sodium chloride, sodium sulfate, potassium dihydrogen phosphate, dipotassium hydrogen phosphate, ammonium chloride were also all procured from Sigma-Aldrich. Paracetamol was purchased from a drugstore, and was ground into powder before dissolution in deionized (DI) water. Al foil was purchased in a supermarket. DI water was obtained from Milli-Q system. Gold film on glass microscope slides of 100 nm thickness and 99.9% purity, prepared by evaporation under vacuum, were purchased from EMF Corporation (USA).

Preparation of artificial urine

An artificial urine solution was prepared as established in previously published papers.¹⁹ The formula is as follows: 1.1 mM lactic acid, 2.0 mM citric acid, 25 mM sodium bicarbonate, 2.5 mM calcium chloride, 90 mM sodium chloride, 2.0 mM magnesium sulfate, 10 mM sodium sulfate, 7.0 mM potassium dihydrogen phosphate, 7.0 mM dipotassium hydrogen phosphate, and 25 mM ammonium chloride in DI water. A concentration series of urea were made up at 600, 400, 200, 100, 50 mM in artificial urine.

Preparation of substrates

An Al substrate was prepared by attaching Al foil onto the glass (cut from microscope slides 1×1 cm) with double-sided scotch. We prepared analyzed solutions of different concentrations, dissolving paracetamol in DI water and

dissolving urea in solution of freshly or recently prepared (stored in refrigerator no longer than 1 – 2 days) artificial urine. A piece of parafilm with a perforated hole of about 5 mm diameter was applied to and briefly heated to 50 – 60°C (for film adhesion) substrates, in order to limit spreading of the drop by its hydrophobic surface. Commercial gold nanoparticles went through 2 or 3 centrifugation/resuspension in water cycles (2500g/10 min for 80 nm diameter), as described in a Gudun *et al.* publication. Next, 25 μ L of the final nanoparticle suspension was dropcasted at the center of each parafilm encircled address at the surface of Al foil or gold film covered glass slide. After drying of the suspension, the prepared analyte solutions (also 25 μ L) were dropcasted onto each prepared substrate and left to dry before Raman measurements.

Apparatus

We used a LABRAM Horiba microscope illuminated with 633 nm at ~ 1.5 mW (for paracetamol) and ~ 3 mW (for urea) He-Ne laser powers. For detection of paracetamol we used a $\times 50$ objective and for detection of urea $\times 10$ objective, while exposure for each datapoint was 3 s for both analytes. Calibration of the microscope was done with the 520 cm^{-1} Si Raman line. The background corrected Raman intensities were averaged from 8 maps, containing 64 datapoint each, for the quantitative detection of paracetamol. The Raman intensity of the amide III band at around 1325 – 1330 cm^{-1} was used for the quantification of paracetamol. For the quantification of urea we used the same symmetrical C–N stretch at around 1012 cm^{-1} as was used by the Cunningham group.¹⁹ For the detection of the urea maximum Raman signal, obtained with a 633-nm laser in the range of 990 to 1020 cm^{-1} was corrected by the subtraction of the fluorescence background (as signal averaged for 965 – 975 cm^{-1} and 1040 – 1050 cm^{-1} ranges) and then averaged from 3 or 4 Raman maps containing 100 (10×10) data points each. For the detection of paracetamol, the range for the maximum signal was 1320 – 1350 cm^{-1} , while the fluorescent background was subtracted from the maximum signal as the average in (1300 – 1310, 1360 – 1370 cm^{-1} ranges). AFM maps were obtained with an AIST atomic force microscope in the tapping mode.

Calculation of LOD and LOQ

The limit of detection (LOD) for paracetamol and for urea is defined as the concentration of analyte at three standard deviations of the blank signal by the following formula:

$$\text{LOD} = 10^{\left(\log \text{LOD} = \frac{3\text{std}-b}{a}\right)}, \quad (1)$$

where 3std is the 3 standard deviation of the blank and a and b are the slope and the intercept of the semi-logarithmic calibration plot, respectively.

The limit of quantification (LOQ) for those analytes is defined as the concentration at 10 std of the blank calculated by a similar formula,

$$\text{LOQ} = 10^{\left(\log \text{LOQ} = \frac{10\text{std}-b}{a}\right)}, \quad (2)$$

where a and b are the same variables as those in formula (1).

Results and Discussion

Detection of paracetamol

The results of paracetamol detection in aqueous solution in

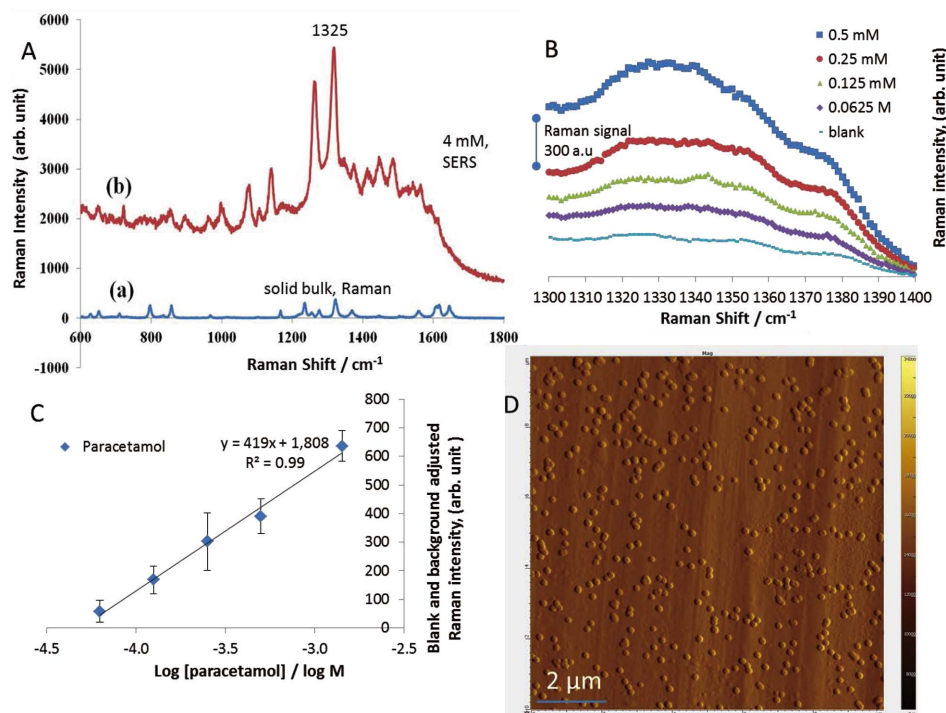


Fig. 1 (A) Raman spectra of solid paracetamol powder (a) and SERS spectrum of 4×10^{-3} mol/L paracetamol dropcasted onto 80 nm AuNPs@AlF. (B) SERS Raman spectra of 0 to 0.5 mM paracetamol solutions on AuNPs@AlF in the range near characteristic vibration. (C) Semi-logarithmic calibration plot for paracetamol solution SERS on AuNPs@AlF. (D) AFM map of 10×10 micron 80 nm AuNPs@AlF substrate in magnification imaging mode.

the concentration range 0.0625 – 1.42 mM are summarized on Fig. 1 below.

Figure 1A shows the Raman spectrum of solid bulk paracetamol (a) and SERS spectrum of paracetamol the 4 mM solution. The characteristic SERS peak at around 1320 cm^{-1} is selected for quantification of SERS Raman signal. Figure 1B shows a zoom in for this characteristic Raman peak recorded from blank, 0.0625, 0.125, 0.25, 0.5 mM solutions of paracetamol. Figure 1C demonstrates a semi-logarithmic calibration plot with background and a blank adjusted Raman signal as a function of the decimal logarithm of paracetamol concentration in the concentration range 0.0625 – 1.42 mM. As shown by $R^2 = 0.99$ on the plot, there is a strong logarithmic dependence of the SERS signal on the concentration in this range. The error bars show standard errors of 8 maps taken for each datapoint on the plot. Using formula (1) with the slope (a) and intercept (b) from the calibration plot equation at Fig. 1C, we calculated. The limit of detection (LOD) for paracetamol on an AuNPs@AlF substrate. This LOD is 0.11 mM, which is about an order of magnitude lower than the LOD reported for paracetamol SERS detection on a gold nanoparticle-chitosan substrate.²² We also calculated the LOQ, using formula (2) and the same standard deviation of the blank, slope and intercept. The LOQ for paracetamol is 0.7 mM

AFM mapping of the AuNPs@AlF substrate with 0.0625 mM paracetamol sample was performed to evaluate the degree of nanoparticle association in the assay. We found from the NP count on four $10 \times 10 \mu\text{m}$ AFM maps that only $43 \pm 4\%$ of all observed nanoparticles on average were singles and all of the rest of NPs were associated in dimers, trimers and oligomers. This finding falls in line with the observation of 50 – 70% nanoparticle association observed with AFM mapping/data

analysis for human IgG SERS sandwich immunoassays, as reported by Sergiienko *et al.*²³

Detection of urea in artificial urine

A plot of the Raman signal vs. Stokes shift in the range 800 to 1200 cm^{-1} as well as the same plots in the limited range $990 - 1040 \text{ cm}^{-1}$ for detection of urea in artificial urine on each of 3 substrates (AuNPs at Au film or Al foil or glass) as well as a calibration plot of Raman signal vs. logarithm of the urea concentration are shown in Fig. 2 below.

The data used for calculation of the LOD and LOQ in detection/quantification of urea are shown for the above mentioned substrates in Table 1 below.

From the second column in Table 1 above it is evident that semi logarithmic calibration (signal vs. $\log[\text{urea}]$) works much better, showing an R^2 closer to the perfect $R^2 = 1$, in comparison to linear (signal vs. $[\text{urea}]$) calibration for the detection of urea with all 3 tested substrates. The R^2 coefficients for a semi-logarithmic calibration are 0.938, 0.983 and 0.917 for Au film, Al foil and glass, respectively, while for linear calibration the R^2 coefficients are 0.856, 0.918 and 0.785, respectively. Therefore, for calculating the limit of detection, we used semi logarithmic calibration, which is a common calibration type for many bioanalytical applications of SERS, such as the label free detection of target DNA by Gao *et al.*²⁴ The limit of detection decreasing in the row AuNPs on gold, Al foil, glass, but LOD for gold and Al foil are not that much different (17 and 24 mM, respectively) in comparison to the LOD for urea on AuNPs@glass of 42 mM. An assay done with AuNPs@glass, not only much lagging behind in linearity ($R^2 = 0.917$), but works in very limited urea concentration range from 50 to 200 mM, because the signal for 400 mM of urea is about the same, namely 294

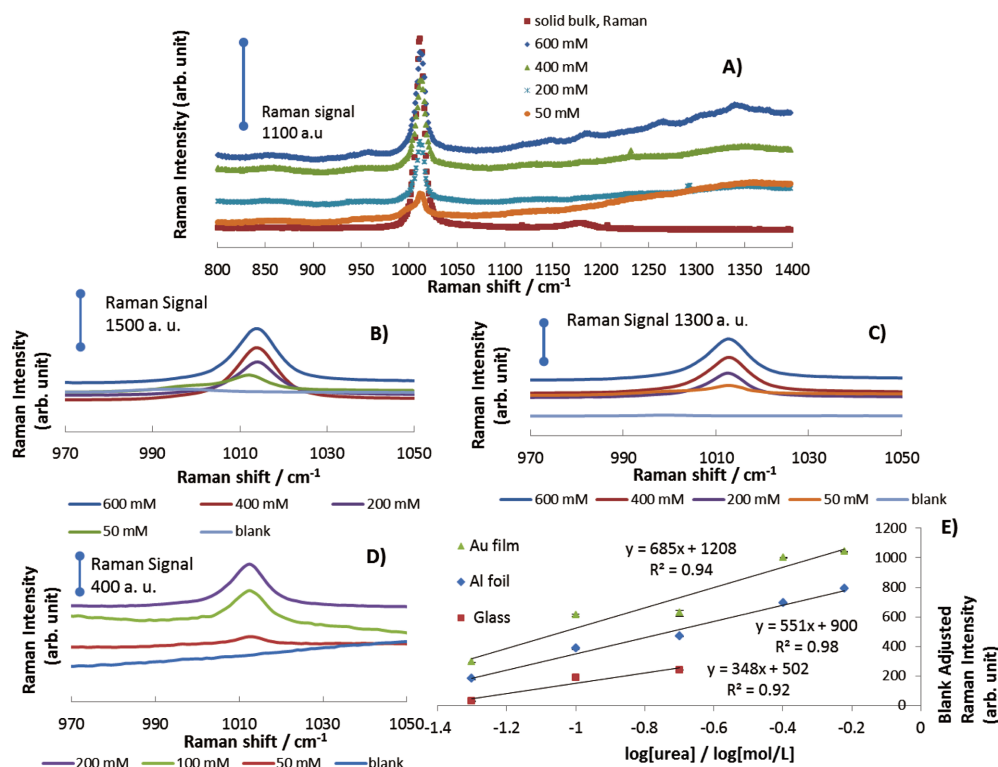


Fig. 2 (A) Raman spectra of urea solid bulk and SERS for different concentrations of urea detected with 60 nm AuNPs@AlF substrate. (B)–(D) are Raman spectra of various concentrations of urea detected with AuNPs on Au film, Al foil, and glass, respectively. (E) Plot of the blank adjusted maximum Raman signal *versus* the logarithm of urea concentration ($\log[\text{urea}]$), obtained on AuNPs@ Au film, AuNPs@AlF, AuNPs@glass substrates

Table 1 Results of SERS quantification of urea in artificial urine with 60 nm commercial gold nanoparticles at three substrates: AuNPs@ Au film, AuNPs@Al foil and AuNPs@glass

Substrate	R^2 semi-logarithmic/linear	Slope for Raman intensity vs. $\log[\text{urea}]$	LOD/mM	LOQ/mM	Concentrations used for LOD calculation/mM	Average background corrected Raman intensity (arb. unit)	Standard error of Raman intensity (arb. unit)
AuNPs/Au film	0.938/0.856	685	17	18	600	1090	4
					400	1048	3
					200	672	24
					100	659	8
					50	343	1
					Blank	49	
AuNPs/Al foil	0.983/0.918	551	24	26	600	813	2
					400	713	2
					200	489	1
					100	405	4
					50	203	4
					Blank	24	1
AuNPs/glass	0.917/0.785	348	42	57	400 ^a	294 ^a	4
					200	295	1
					100	245	4
					50	86	3
					Blank	56	4

a. Outside of the calibration trendline range.

a.u., as the signal for 200 mM concentration in the assay on glass. Clearly, unlike Al foil and gold film, glass is not a satisfactory component of the SERS substrate to detect urea in urine at a clinically relevant concentration range. However, an assay on Au film demonstrates that $R^2 = 0.938$, which is not

nearly as high as $R^2 = 0.983$ for an assay with Al foil. Here, AuNPs@Al foil performs significantly better than AuNPs@Au film, since $(1 - R^2)$ for calibration on Al foil is almost 3 fold lower than $(1 - R^2)$ for calibration on Au film, while both semi-log trendlines for urea are shown at Fig. 2E. As we calculated

recoveries for all 5 standard concentrations of urea in urine on both Al foil and on gold, we also observed that the average absolute deviation of recovery from 100% ($\text{abs}[100\% - \text{recovery}\%]$) for the assay on AuNPs@Al foil is nearly 3-fold smaller (7.7%) than the average absolute deviation of recovery from 100% for the assay on AuNPs@gold (20%). Since urea's LOQ of 26 mM obtained with AuNPs@Al foil is below the lowest pathophysiological concentration of 0.03 M for urea in urine, there is hardly any significant advantage in using more expensive, more sensitive to contamination and less available gold film instead of ubiquitous untreated Al foil in tandem with commercial gold nanoparticles for the quantification of urea in urine.

Conclusions

We demonstrated that commercial gold nanoparticles at Al foil can successfully compete with gold nanoparticles at gold film as a SERS substrate in detection of the important biomarker urea near the ranges of the pathological and normal concentration of urea in human urine, achieving LOD of 24 mM and LOQ of 26 mM, which is about 1/13 of the average concentration, and which is below the lowest pathophysiological concentration of urea in urine. Overall, it appears that AuNPs@AlF may become a substrate of choice for the cost-efficient and fast SERS detection of urea in urine. Moreover, this low-cost and easily prepared substrate can detect paracetamol as an example of the pharmaceutical/environment pollutant at fairly low concentration. The LOD for SERS of paracetamol on AuNP@AlF is about 9-times lower than the lowest reported LOD of 1 mM detected with SERS spectroscopy method, to the best of our knowledge.²²

References

1. M. Fleischmann, P. J. Hendra, and A. J. McQuillan, *Chem. Phys. Lett.*, **1974**, 26, 163.
2. K. Kim and K. S. Shin, *Anal. Sci.*, **2011**, 27, 775.
3. H. Nakao, *Anal. Sci.*, **2014**, 30, 151.
4. K. C. Bantz, A. F. Meyer, N. J. Wittenberg, H. Im, Ö. Kurtuluş, S. H. Lee, N. C. Lindquist, S. H. Oh, and C. L. Haynes, *Phys. Chem. Chem. Phys.*, **2011**, 13, 11551.
5. M. D. Porter, R. J. Lipert, L. M. Siperko, G. Wang, and R. Narayanan, *Chem. Soc. Rev.*, **2008**, 37, 1001.
6. X. Zhang, M. A. Young, O. Lyandres, and R. P. Van Duyne, *J. Am. Chem. Soc.*, **2005**, 127, 4484.
7. D. S. Grubisha, R. J. Lipert, H. Y. Park, J. Driskell, and M. D. Porter, *Anal. Chem.*, **2003**, 75, 5936.
8. J. C. Love, L. A. Estroff, J. K. Kriebel, R. G. Nuzzo, and G. M. Whitesides, *Chem. Rev.*, **2005**, 105, 1103.
9. R. Bukasov, T. A. Ali, P. Nordlander, and J. S. Shumaker-Parry, *ACS Nano*, **2010**, 4, 6639.
10. M. D. Malinsky, K. L. Kelly, G. C. Schatz, and R. P. Van Duyne, *J. Am. Chem. Soc.*, **2001**, 123, 1471.
11. W. W. Yu and I. M. White, *Analyst*, **2012**, 137, 1168.
12. M.-L. Zhang, X. Fan, H.-W. Zhou, M.-W. Shao, J. A. Zapien, N.-B. Wong, and S.-T. Lee, *J. Phys. Chem. C*, **2010**, 114, 1969.
13. S. Mabbott, A. Eckmann, C. Casiraghi, and R. Goodacre, *Analyst*, **2013**, 138, 118.
14. M. M. Martinez-Garcia, P. E. Cardoso-Avila, and J. L. Pichardo-Molina, *Colloids Surf.*, **2016**, 493, 66.
15. K. Gudun, Z. Elemessova, L. Khamkhash, E. Ralchenko, and R. Bukasov, *J. Nanomater.*, **2017**, Article ID 9182025.
16. A. Radomska, R. Koncki, K. Pyrzyńska, and S. Głab, *Anal. Chim. Acta*, **2004**, 523, 193.
17. N. R. Hill, S. T. Fatoba, J. L. Oke, J. A. Hirst, C. A. O'Callaghan, D. S. Lasserson, and F. D. R. Hobbs, *Plos One*, **2016**, 11, e0158765.
18. T.-L. Wang, H. K. Chiang, H.-H. Lu, and F.-Y. Peng, *Opt. Quantum Electron.*, **2005**, 37, 1415.
19. C. J. Choi, H.-Y. Wu, S. George, J. Weyhenmeyer, and B. T. Cunningham, *Lab Chip*, **2012**, 12, 574.
20. L. Liu, H. Mo, S. Wei, and D. Raftery, *Analyst*, **2012**, 137, 595.
21. K. Klimova and J. Leitner, *Thermochim. Acta*, **2012**, 550, 59.
22. E. D. Santos, E. C. N. L. Lima, C. S. de Oliveira, F. A. Sigoli, and I. O. Mazali, *Anal. Methods*, **2014**, 6, 3564.
23. S. Sergiienko, K. Moor, K. Gudun, Z. Yelemessova, and R. Bukasov, *Phys. Chem. Chem. Phys.*, **2017**, 19, 4478.
24. F. Gao, J. Lei, and H. Ju, *Anal. Chem.*, **2013**, 85, 11788.